Structural Engineering and Mechanics, Vol. 6, No. 2 (1998) 201-215
DOI: http://dx.doi.org/10.12989/sem.1998.6.2.201

Discontinuous deformation analysis for reinforced concrete frames infilled with masonry walls

Yaw-Jeng Chiou†, Jyh-Cherng Tzeng‡ and Shuenn-Chang Hwang‡

Department of Civil Engineering, National Cheng-Kung University, Tainan, Taiwan 701, R.O.C.

Abstract. The structural behavior of reinforced concrete frame infilled with a masonry wall is investigated by the method of discontinuous deformation analysis (DDA). An interface element is developed and it is incorporated into DDA to analyze the continuous and discontinuous behavior of the masonry structure. The numerical results are compared with previous research and possess satisfactory agreement. Then the structural behavior and stress distribution of a reinforced concrete frame infilled with a masonry wall subjected to a horizontal force are studied. In addition, the justification of equivalent strut is assessed by the distribution of principal stresses. The results show that the behavior of the masonry structure is highly influenced by the failure of mortar. On the basis of the distribution of principal stress of the masonry wall in the reinforced concrete frame, the equivalent strut can be approximately substituted for the masonry wall without separation and opening. However, the application of equivalent strut to the masonry wall with separation and opening needs further study.

Key words: discontinuous deformation analysis; reinforced concrete building; masonry wall.

1. Introduction

The reinforced concrete frames infilled with masonry walls have been widely used for building constructions. The masonry walls are constructed with brittle materials and the failure of which is frequently initiated from the cracking of mortar and separation of brick. Structure failure induced by cracking and separation causes existence of discontinuous and nonlinear behavior.

Smith (1966) examined the behavior of infilled frames by the finite difference method and adopted a simplified equivalent single strut model to replace the wall. The equivalent strut model has been widely used by engineers and researchers. Liauw (1972) proposed an equivalent frame method to analyze the infilled frames. Thiruvengadam (1985) used the finite element method, the equivalent single strut model, and the equivalent multiple strut model to study the natural frequencies of infilled frames with opening and separation of wall. Achyutha, *et al.* (1986) proposed an iterative finite element method of analysis to simulate the elastic behavior of infilled frames with and without opening. Ali and Page (1988) studied the stress distributions and failure behaviors of masonry structures by the finite element method. Alternatively, Papia (1988) proposed a coupled finite element and boundary element method to analyze the infilled frames. The analysis was carried out by using the boundary element method for the infill and op-

† Professor
‡ Graduate Students

portunely divided the frame into the finite element. Dawe and Seah (1989a, b) investigated the behavior of masonry infilled steel frames experimentally by using large-scale specimens and scale models. In addition, they compared the experimental dynamic results with those of the three analytical models--the single degree of freedom model, the braced frame model, and the equivalent strut model. They pointed out that the analytical result of equivalent strut model was found to be unsatisfactory in predicting dynamic response of masonry infilled frames. Gulkan, *et al.* (1990) and Clough, *et al.* (1990) studied the earthquake response of masonry structures by the method of seismic testing. Similar study was presented by Abrams and Paulson (1991). Lotfi and Shing (1991) studied the masonry shear wall by incorporating the smeared crack models into the method of finite element. El Haddad (1991) studied the cracking and stress redistribution of infilled frames based on the finite element method and fracture mechanics techniques. May and Naji (1991) developed a nonlinear finite element method to simulate the behavior of steel frames infilled with concrete panels subjected to monotonic or cyclic loading. Mehrabi (1994) evaluated the safety of existing masonry infilled reinforced concrete structures under earthquake loadings by using the half-scale specimen experiment and finite element method. Recently, Saneinejad and Hobbs (1995) developed an inelastic analysis and design method for infilled steel frames subjected to in-plane forces. More recently, Haider (1996) studied the in-plane cyclic response of reinforced concrete frames with unreinforced masonry infill by the full-scale specimen experiment and the equivalent strut model.

The cracking and separation phenomena occurring in the masonry structures cause distinct block elements. As a result, the masonry structures characterize discontinuous and nonlinear behavior. The nature and orientation of discrete blocks play an important role in the performance of masonry structures. To model the masonries as discrete blocks by the classical numerical methods (finite difference method, finite element method, and boundary element method) is not an easy task and is usually very time consuming. Recently, El Shabrawi and Verdel (1995) applied the distinct element method (DEM, Cundall 1971) to study the behavior of ancient masonry structures under dynamic loads. The DEM has been proved to be indispensable to many engineers in approaching rock analysis. Because fractured rock masses and masonry building are similar in nature of materials, the use of the DEM is justified. However, the DEM employs an explicit central difference time-marching scheme to integrate the equation of motion directly (Cundall and Hart 1989). Since a central difference procedure is conditionally stable, the time-step size must not exceed a critical value. As a result, the computation time used in DEM is dramatically large even for a simple problem. Moreover, a mathematical damping is used in DEM to dissipate the extra kinetic energy, and the current block kinematics in DEM can not handle complex contact situations such as corner-corner contacts. Because of its incomplete block kinematics and mathematical damping, the explicit scheme used in DEM can not guarantee the dynamic equilibrium state of a system at any time. Alternatively, Shi (1988) proposed the method of discontinuous deformation analysis (DDA). DDA is an implicit method, in which displacements are the unknowns to be solved. Shi (1988) addressed five unique features of DDA:

(1) complete block kinematics and its numerical realization;
(2) perfect first-order displacement approximation;
(3) strict postulate of equilibrium;
(4) correct energy consumption; and
(5) high computing efficiency.

The first four features make DDA a rigorous analysis for discrete blocks. This method has been adopted and extended by some researchers (Shyu 1993, Ke 1993, Chang 1994, Lin 1995).

This study applied DDA to investigate the structure behavior of masonry structures. The prototype of DDA can study the discontinuous deformation of block system efficiently. However, the masonry wall behaves as a continuous structure if the mortar is not cracked. An interface element is developed and is incorporated into DDA to analyze the continuous and discontinuous behaviors of masonry structure. The proposed numerical method is first verified by comparing the present results with previous research. Then the structural behavior and stress distribution of infilled frames with or without opening are fully studied. In addition, the justification of equivalent strut is assessed by the distribution of principal stresses.

2. Problem formulation

In the method of discontinuous deformation analysis (DDA, Shi 1988), the variables are displacements and the equilibrium equations are solved in the same way as finite element method does. However, DDA does not imply continuity at block boundaries. The blocks are independent and they only have connections while in contact with one another. These connections are performed by adding springs to the contacting positions. The compatibility conditions for the block systems are no-tension and no-penetration between any two blocks. These two constraints are inequalities in mathematical forms. However, the blocks are in contact only along the block boundaries so these inequalities can be transformed into a set of equalities upon which the equilibrium equations can be set up and solved. A complete first order polynomial is chosen as the displacement function for a two-dimensional block, and this displacement function restricts the block to constant stress.

Referring to Fig. 1, the displacements (u, v) of any point (x, y) in a representative block i (Shi 1988) are given as

$$\begin{Bmatrix} u \\ v \end{Bmatrix} = \begin{bmatrix} 1 & 0 & -(y-y_0) & (x-x_0) & 0 & (y-y_0)/2 \\ 0 & 1 & (x-x_0) & 0 & (y-y_0) & (x-x_0)/2 \end{bmatrix} \begin{Bmatrix} u_0 \\ v_0 \\ r_0 \\ \varepsilon_x \\ \varepsilon_y \\ \gamma_{xy} \end{Bmatrix} \tag{1a}$$

or

$$\begin{Bmatrix} u \\ v \end{Bmatrix} = [\boldsymbol{T}_i]\,[\boldsymbol{D}_i] \tag{1b}$$

where (x_0, y_0) are the coordinates of block centroid, $[\boldsymbol{T}_i]$ is the first order displacement function, $[\boldsymbol{D}_i]^T = (u_0, v_0, r_0, \varepsilon_x, \varepsilon_y, \gamma_{xy})_i$ is the displacement vector of block i, (u_0, v_0) are the rigid body translation, r_0 is the rigid body rotation, and $(\varepsilon_x, \varepsilon_y, \gamma_{xy})$ are the strain components in a two-dimensional geometry. By minimizing the total potential energy, the equilibrium equations for n blocks (Shi 1988) are

$$\begin{bmatrix} \boldsymbol{K}_{11} & \boldsymbol{K}_{12} & \boldsymbol{K}_{13} & \cdots & \boldsymbol{K}_{1n} \\ \boldsymbol{K}_{21} & \boldsymbol{K}_{22} & \boldsymbol{K}_{23} & \cdots & \boldsymbol{K}_{2n} \\ \boldsymbol{K}_{31} & \boldsymbol{K}_{32} & \boldsymbol{K}_{33} & \cdots & \boldsymbol{K}_{3n} \\ \vdots & \vdots & \vdots & \vdots & \vdots \\ \boldsymbol{K}_{n1} & \boldsymbol{K}_{n2} & \boldsymbol{K}_{n3} & \cdots & \boldsymbol{K}_{nn} \end{bmatrix} \begin{Bmatrix} \boldsymbol{D}_1 \\ \boldsymbol{D}_2 \\ \boldsymbol{D}_3 \\ \vdots \\ \boldsymbol{D}_n \end{Bmatrix} = \begin{Bmatrix} \boldsymbol{F}_1 \\ \boldsymbol{F}_2 \\ \boldsymbol{F}_3 \\ \vdots \\ \boldsymbol{F}_n \end{Bmatrix} \tag{2}$$

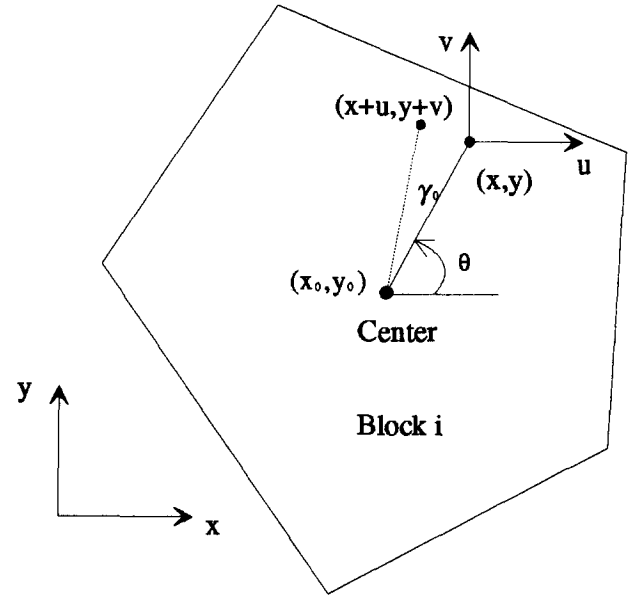

Fig. 1 Schematic configuration of a block.

where $\boldsymbol{K}_{ij}$ is the component of stiffness matrix, $\boldsymbol{K}_{ij}$ depends on the material modulus and inertia effect of block i, $\boldsymbol{K}_{ij}$ $(i \neq j)$ depends on the contacts or bolt connection between block i and block j, $\boldsymbol{D}_i$ is the displacement vector of block i, and $\boldsymbol{F}_i$ is the force vector of block i.

To analyze the continuous behavior of masonry structures, an interface element is proposed in this study. Referring to Fig. 2, a constant stress triangular element is adopted as the interface element. The three nodes are connected to blocks i, j, and k, respectively. The shape functions are

$$\begin{aligned} \hat{\psi}_1 &= L_1 \\ \hat{\psi}_2 &= L_2 \\ \hat{\psi}_3 &= L_3 = 1 - L_1 - L_2 \end{aligned} \tag{3}$$

where Li $(i=1, 2, 3)$ represent the area coordinates. The interpolations of the displacement field and coordinates are written as

$$\begin{aligned} u &= \sum_{n=1}^{3} u_n \hat{\psi}_n \\ v &= \sum_{n=1}^{3} v_n \hat{\psi}_n \end{aligned} \tag{4}$$

$$\begin{aligned} x &= \sum_{n=1}^{3} x_n \hat{\psi}_n \\ y &= \sum_{n=1}^{3} y_n \hat{\psi}_n \end{aligned} \tag{5}$$

where (u_n, v_n) and (x_n, y_n) are the nodal displacements and nodal coordinates, respectively. The nodal displacements can be calculated by putting the nodal coordinates into Eq. (1). By putting the nodal displacements in Eq. (4), the displacement field is thus obtained as follows.

$$\begin{Bmatrix} u \\ v \end{Bmatrix} = \begin{bmatrix} [T_1^i]\hat{\psi}_1 & [T_1^j]\hat{\psi}_2 & [T_1^k]\hat{\psi}_3 \\ [T_2^i]\hat{\psi}_1 & [T_2^j]\hat{\psi}_2 & [T_2^k]\hat{\psi}_3 \end{bmatrix} \begin{Bmatrix} [D_i] \\ [D_j] \\ [D_k] \end{Bmatrix} \tag{6}$$

where $[T_1^i]$ and $[T_2^i]$ represent the partitioned components of the first order displacement function $[T_i]$. The strain components of the interface element are

$$\begin{Bmatrix} \varepsilon_x \\ \varepsilon_y \\ \gamma_{xy} \end{Bmatrix} \begin{bmatrix} \dfrac{\partial u}{\partial x} \\ \dfrac{\partial v}{\partial y} \\ \dfrac{1}{2}\left(\dfrac{\partial u}{\partial y} + \dfrac{\partial v}{\partial x}\right) \end{bmatrix} =$$

$$\begin{bmatrix} [T_1^i]\dfrac{\partial \hat{\psi}_1}{\partial x} & [T_1^j]\dfrac{\partial \hat{\psi}_2}{\partial x} & [T_1^k]\dfrac{\partial \hat{\psi}_3}{\partial x} \\ [T_2^i]\dfrac{\partial \hat{\psi}_1}{\partial y} & [T_2^j]\dfrac{\partial \hat{\psi}_2}{\partial y} & [T_2^k]\dfrac{\partial \hat{\psi}_3}{\partial y} \\ \dfrac{1}{2}\left([T_1^i]\dfrac{\partial \hat{\psi}_1}{\partial y} + [T_2^i]\dfrac{\partial \hat{\psi}_1}{\partial x}\right) & \dfrac{1}{2}\left([T_1^j]\dfrac{\partial \hat{\psi}_2}{\partial y} + [T_2^j]\dfrac{\partial \hat{\psi}_2}{\partial x}\right) & \dfrac{1}{2}\left([T_1^k]\dfrac{\partial \hat{\psi}_3}{\partial y} + [T_2^k]\dfrac{\partial \hat{\psi}_3}{\partial x}\right) \end{bmatrix} \begin{Bmatrix} [D_i] \\ [D_j] \\ [D_k] \end{Bmatrix} \tag{7}$$

The stiffness matrix and force vector of the interface element are derived by using the principle of minimum potential energy. The strain energy π_e of element is described as

$$\pi_e = \frac{1}{2}\int_0^1 \int_0^{1-L_1} [\varepsilon_x \ \varepsilon_y \ \gamma_{xy}][E] \begin{Bmatrix} \varepsilon_x \\ \varepsilon_y \\ \gamma_{xy} \end{Bmatrix} |J| \, dL_1 \, dL_2$$

$$= \frac{|J|}{4} [[D_i]^T \ [D_j]^T \ [D_k]^T] \begin{bmatrix} [B_{11}] & [B_{12}] & [B_{13}] \\ [B_{21}] & [B_{22}] & [B_{23}] \\ [B_{31}] & [B_{32}] & [B_{33}] \end{bmatrix} \begin{Bmatrix} [D_i] \\ [D_j] \\ [D_k] \end{Bmatrix} \tag{8}$$

where

$$|J| = \begin{vmatrix} x_1 - x_3 & y_1 - y_3 \\ x_2 - x_3 & y_2 - y_3 \end{vmatrix} \tag{9}$$

After taking derivatives with respect to displacement variables from the strain energy π_e of the element, the components of stiffness matrix are obtained as

$$[K_{ii}] = \frac{|J|}{2}[B_{11}],\ [K_{jj}] = \frac{|J|}{2}[B_{22}],\ [K_{kk}] = \frac{|J|}{2}[B_{33}]$$
$$[K_{ij}] = \frac{|J|}{4}([B_{21}]^T + [B_{12}]),\ [K_{ik}] = \frac{|J|}{4}([B_{31}]^T + [B_{13}])$$
$$[K_{jk}] = \frac{|J|}{4}([B_{32}]^T + [B_{23}]),\ [K_{ji}] = \frac{|J|}{4}([B_{21}] + [B_{12}]^T)$$
$$[K_{ki}] = \frac{|J|}{4}([B_{31}] + [B_{13}]^T),\ [K_{kj}] = \frac{|J|}{4}([B_{32}] + [B_{23}]^T) \tag{10}$$

The stiffness matrix of the interface element is added to the corresponding components of global stiffness matrix in Eq. (2) to modify the DDA method. The solution procedures of DDA are divided into many steps; there are initial stresses (σ_x^0, σ_y^0, τ_{xy}^0) existing in each time step. The strain energy π_σ induced by the initial stresses is

$$\pi_\sigma = \int_0^1 \int_0^{1-L_1} [\varepsilon_x\ \varepsilon_y\ \gamma_{xy}] \begin{Bmatrix} \sigma_x^0 \\ \sigma_y^0 \\ \tau_{xy}^0 \end{Bmatrix} dx\, dy$$
$$= \frac{|J|}{2}[[D_i]^T\ [D_j]^T\ [D_k]^T] \begin{Bmatrix} [P_1] \\ [P_1] \\ [P_3] \end{Bmatrix} \tag{11}$$

Similar to the derivation of stiffness matrix, the force vector induced by the initial stresses is derived by taking derivatives with respect to displacement variables from the strain energy π_σ.

$$[F_i] = -\frac{|J|}{2}[P_1]$$
$$[F_j] = -\frac{|J|}{2}[P_2]$$
$$[F_k] = -\frac{|J|}{2}[P_3] \tag{12}$$

The force vector is also added to the corresponding components of global force vector Eq. (2) to modify the DDA method. The implementation of interface element for analysis of masonry and concrete structures is shown in Fig. 3. Referring to Fig. 3a, one can see that the brick is modeled as a block element, and the interface element is adopted to model the mortar. On the analysis of reinforced concrete structure, referring to Fig. 3b, the concrete is divided into block elements and the blocks are connected by the interface element. In addition, the reinforced steel is modeled by the interface element.

The failure of mortar is determined either by its tensile strength or shear strength. The shear strength is characterized by the Mohr-Coulomb failure criterion.

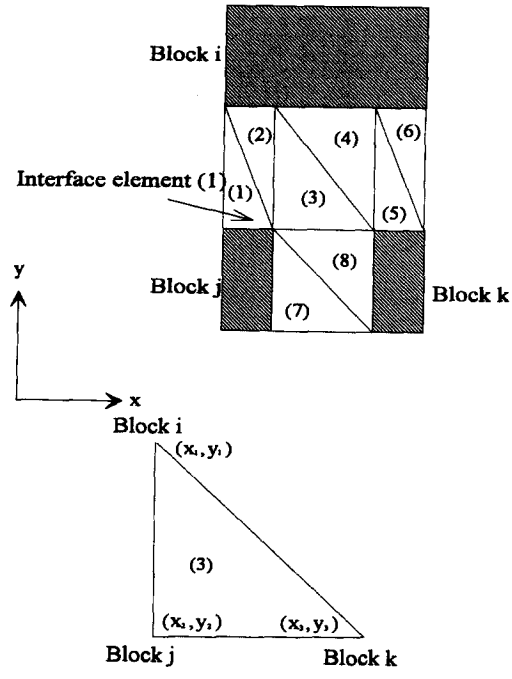

Fig. 2 Interface elements.

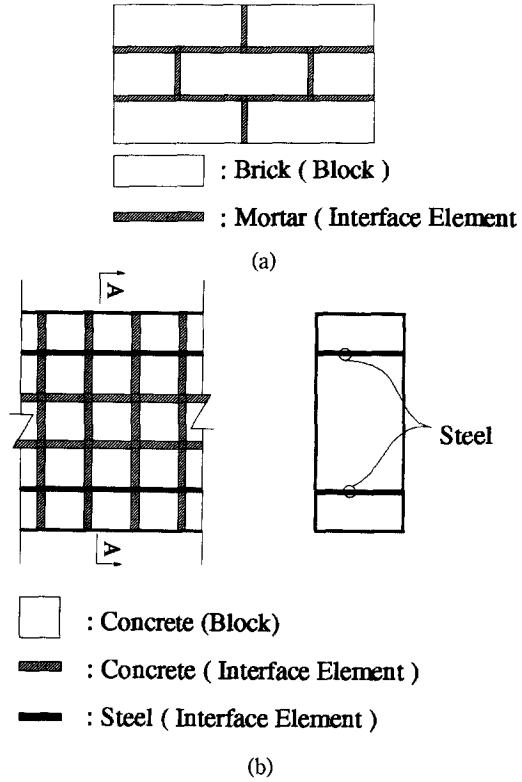

Fig. 3 (a) Schematic configuration of element mesh of the masonry wall, (b) schematic configuration of element mesh of the reinforced concrete structure.

$$\tau = \tau_0 \pm \sigma_n \tan(\phi) \tag{13}$$

where τ_0 is the cohesion, σ_n is the normal stress, and ϕ is the internal friction angle. On the study of reinforced concrete structure, the structure is assumed to be plane stress. The constitutive relations for the uncracked concrete in the prefracture regime are developed based on the isotropic linearly elastic material, while the stress-strain relations of fractured concrete are developed by using the model of smeared cracking approach (Chen and Saleeb 1982). The incremental stress-strain relations for the uncracked concrete are

$$\begin{Bmatrix} d\sigma_x \\ d\sigma_y \\ d\gamma_{xy} \end{Bmatrix} = [E] \begin{Bmatrix} d\varepsilon_x \\ d\varepsilon_y \\ d\gamma_{xy} \end{Bmatrix} \tag{14}$$

where

$$[E] = \frac{E}{(1-\nu^2)} \begin{bmatrix} 1 & \nu & 0 \\ \nu & 1 & 0 \\ 0 & 0 & (1-\nu)/2 \end{bmatrix} \tag{15}$$

E is Young's modulus, ν is Poisson's ratio. The total change in stresses after the formation of cracks (Chen and Saleeb 1982) is

$$\begin{Bmatrix} \Delta\sigma_x \\ \Delta\sigma_y \\ \Delta\tau_{xy} \end{Bmatrix} = [E[b(\psi)][b(\psi)]^T] \begin{Bmatrix} d\varepsilon_x \\ d\varepsilon_y \\ d\gamma_{xy} \end{Bmatrix} - [[I] - [b(\psi)][b'(\psi)^T]] \begin{Bmatrix} \sigma_x \\ \sigma_y \\ \tau_{xy} \end{Bmatrix} \tag{16}$$

where σ_x, σ_y, τ_{xy} are the current stress components at the point just prior to the formation of a crack, and

$$[b(\psi)] = \begin{Bmatrix} \cos^2(\psi) \\ \sin^2(\psi) \\ \cos(\psi)\sin(\psi) \end{Bmatrix}, \quad [b'(\psi)] = \begin{Bmatrix} \cos^2(\psi) \\ \sin^2(\psi) \\ 2\cos(\psi)\sin(\psi) \end{Bmatrix} \quad [I] = \begin{bmatrix} 1 & 0 & 0 \\ 0 & 1 & 0 \\ 0 & 0 & 1 \end{bmatrix} \tag{17}$$

in which ψ is the angle between the cracked direction and x-axis.

3. Results and discussion

The modified DDA method is verified first by comparing the current numerical results with previous research. Fig. 4 shows a masonry wall constructed with 71 bricks (Ali and Page 1988). The dimension of a brick is 4.5 in × 1.5 in × 2.1 in (or 11.43 cm × 3.81 cm × 5.33 cm), and the thickness of mortar is 0.2 in (or 0.51 cm). The tensile strength of the mortar is 42 psi (or 289.38 kN/m^2), and the shear strength depends on the status of the normal stress σ_n.

$$\tau = -0.66\sigma_n + 25.58 \qquad 42 \text{ psi} > \sigma_n \geq 0 \tag{18}$$

$$\tau = -0.87\sigma_n + 25.58 \qquad 0 > \sigma_n \geq -334 \text{ psi} \tag{19}$$

$$\tau = -0.11\sigma_n + 281.42 \qquad -334 \text{ psi} > \sigma_n \tag{20}$$

or

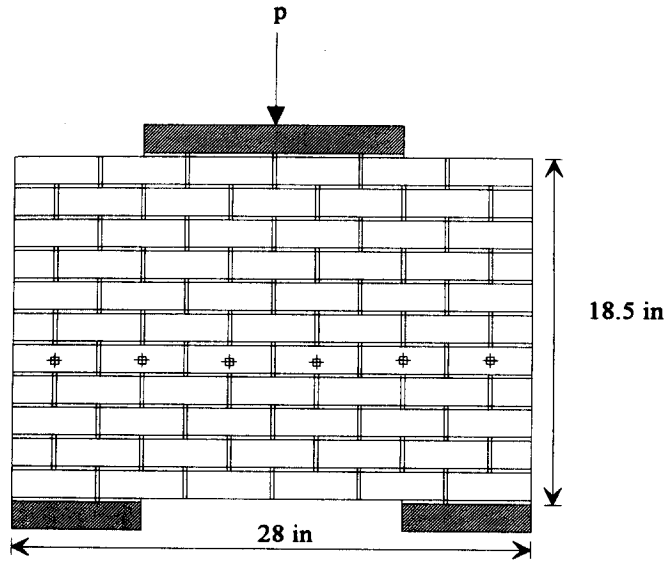

Fig. 4 Schematic configuration of a masonry wall (Ali and Page 1988).

$$\tau = -0.66\sigma_n + 0.176 \qquad 0.289 \text{ N/mm}^2 > \sigma_n \geq 0 \tag{21}$$

$$\tau = -0.87\sigma_n + 0.176 \qquad 0 > \sigma_n \geq -2.3 \text{ N/mm}^2 \tag{22}$$

$$\tau = -0.11\sigma_n + 1.94 \qquad -2.3 \text{ N/mm}^2 > \sigma_n \tag{23}$$

Referring to Fig. 4, the bricks of the masonry wall are modeled as block elements, while the interface elements are used to model the mortar. The failure of the mortar is determined either by its tensile strength or shear strength in Eq. (18)-(20) or Eqs. (21)-(23). The block kinematics used in DDA is adopted. The distributions of vertical normal stress σ_y of fifth layer and comparison of current result with those by Ali and Page (1988) are shown in Fig. 5. Note that the layers are numbered from the bottom up, and the distance X is measured from the left edge. The failure of the masonry wall predicted by this study is shown in Fig. 6. Referring to Fig. 5, one can see that the stresses calculated by the currently modified DDA method agree well with the experimental measured values. In addition, referring to Fig. 5, there is a sharp rise in normal stress. This high stress state is caused by the failure of mortar (Fig. 6), and the failure of mortar induces the discontinuous and nonlinear structure behavior.

Referring to Fig. 7, a RC beam was studied by the finite element method and the experimental method (Suidan and Schnobrich 1973). This RC beam is analyzed by the currently modified DDA method. Half of this beam is divided into 418 blocks and the element mesh is shown in Fig. 8. The load-deflection relation and comparison of present results with those by Suidan and Schnobrich (1973) are shown in Fig. 9. Referring to Fig. 9, it is found that the current results agree well with the experimental result. The discrepancy between the current result and the experimental result increases for the RC beam with yielding of reinforced steel. This discrepancy is induced by the rapid growth of depth of crack penetration and complex change of stress after the yielding of steel. The constant stress element can not simulate the complex stress change exactly, but it can be improved by refining the element mesh.

The proposed numerical method is thus demonstrated to be appropriate for the analysis of

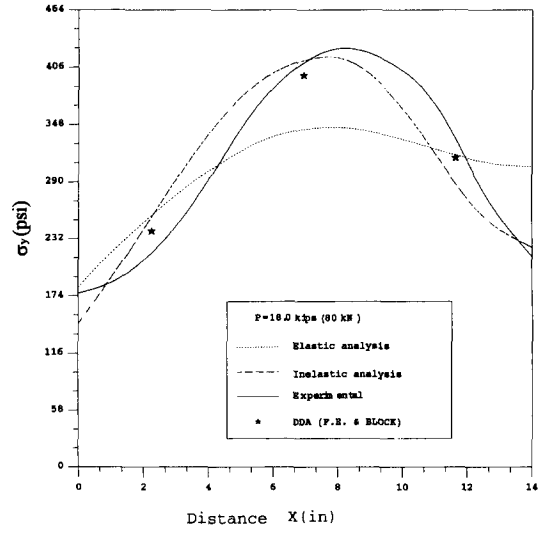

Fig. 5 Comparison of current result with previous research (Ali and Page 1988): Distribution of vertical normal stress σ_y (The distance X is measured from the left edge).

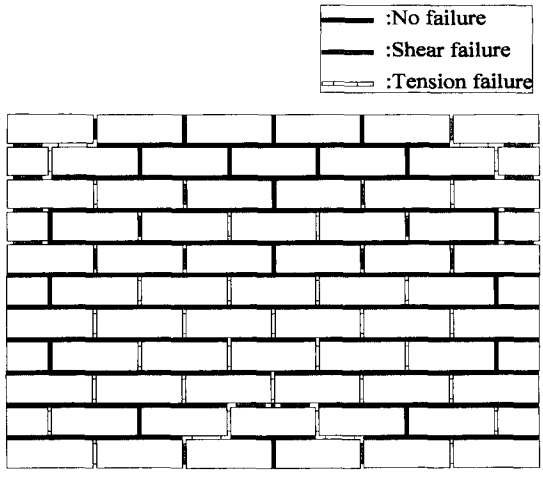

Fig. 6 Failure of masonry wall predicted by the modified DDA method.

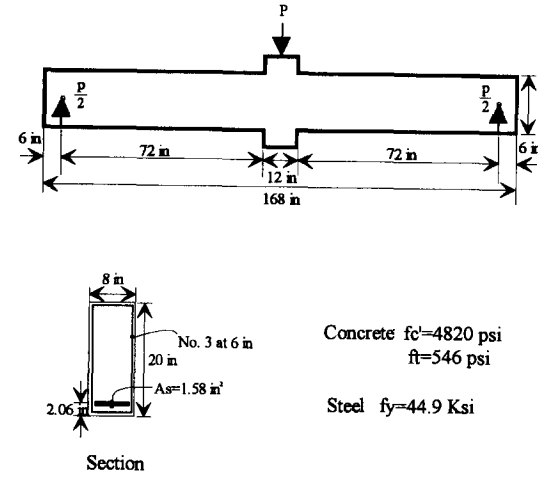

Fig. 7 Schematic configuration of a reinforced concrete beam (Suidan and Schnobrich 1973).

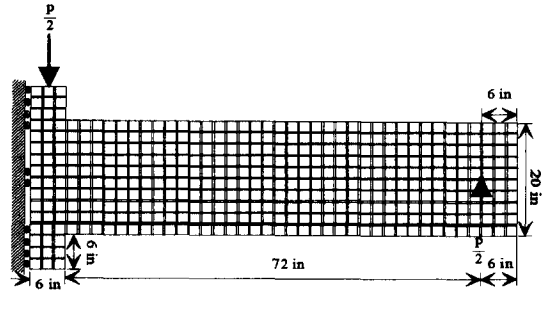

Fig. 8 Element mesh of RC beam (418 blocks).

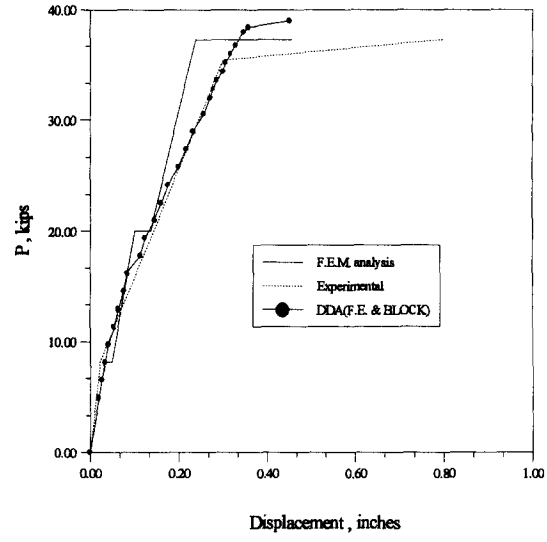

Fig. 9 Comparison of current result with previous research (Suidan and Schnobrich 1973): Load-deflection relation of a RC beam.

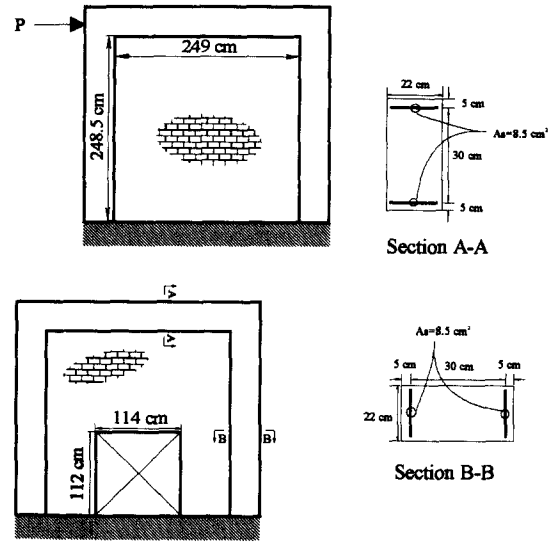

Fig. 10 Layout of the infilled frames.

masonry and reinforced concrete structures. Then the structural behavior of reinforced concrete frame infilled with masonry wall subjected to horizontal force is studied. Both the infilled frames with or without opening are investigated. Fig. 10 shows the layout of the infilled frame. The compressive strength of concrete f_c' is 210 kg/cm^2, the modulus of rupture f_t is 28.98 kg/cm^2, and the yield stress of steel f_y is 2800 kg/cm^2. The size of the brick is 21 cm$\times$5 cm$\times$10 cm, and the thickness of mortar is 1.5 cm. The Young's modulus of brick and mortar are 2.13$\times$10^5 kg/cm^2, and 1.65$\times$10^5 kg/cm^2, respectively. The Poisson's ratio of brick and mortar are 0.165 and 0.17. The tensile resistance of brick-mortar interface is 4.52 kg/cm^2, and the shear resistance is

$$\tau = \tau_0 - \sigma\tan(\phi_1) \quad 4.52\ \text{kg/cm}^2 > \sigma \geq 0 \tag{24}$$

$$\tau = \tau_0 - \sigma\tan(\phi_2) \quad \sigma < 0 \tag{25}$$

where τ_0=9.28 kg/cm^2 is cohesion, ϕ_1=66.13° and ϕ_2=45.29° are the internal frictional angles.

On the analysis of infilled frame, each brick is represented by a block and the reinforced concrete frame is divided into blocks. The adjacent blocks are connected by the interface elements and their separation is determined by the failure analysis. The equivalent diagonal strut (Smith 1966) is investigated by matching the principal direction and the effective region of the equivalent strut defined by the following formulas (Smith 1966).

$$\alpha_h = \frac{\pi}{2}\sqrt[4]{\frac{4E_f I_c h}{E_m t \sin 2\theta}} \tag{26}$$

$$\alpha_L = \pi\sqrt[4]{\frac{4E_f I_b h}{E_m t \sin 2\theta}} \tag{27}$$

where α_h and α_L are the contacted lengths of the equivalent strut to the column and beam, respectively; E_m and E_f represent the elastic moduli of the masonry wall and frame material; t, h, and L are the thickness, height, and length of the infill wall; I_c and I_b are the moments of inertia of the column and the beam of the frame; and θ=tan^{-1} (h/L).

The element mesh of infilled frames without opening of masonry wall is shown in Fig. 11. Fig. 12 shows the distribution of principal stress of this frames if the cracking and separation phenomena are neglected. Referring to Fig. 12, it is found that the principal direction is uniform, and the effective region of the equivalent strut approximately matches the principal direction. The application of the equivalent strut is justified. However, the principal direction of masonry wall is no longer uniform if the cracking and separation of bricks are considered (Fig. 13). Referring to Fig. 13, it is found that the masonry wall is fractured around the upper region and the compressive principal direction tends to be a horizontal one. The equivalent struts seem inapplicable for masonry wall with cracking and separation. Similar study on the stress distribution of masonry wall with opening is shown in Figs. 14-15. Fig. 14 shows the element mesh of this

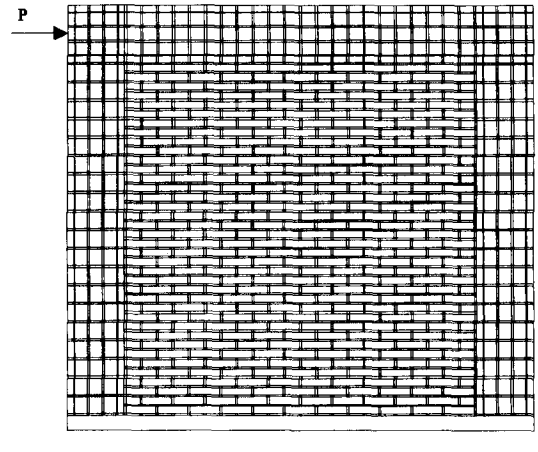

Fig. 11 Element mesh of infilled frame without opening.

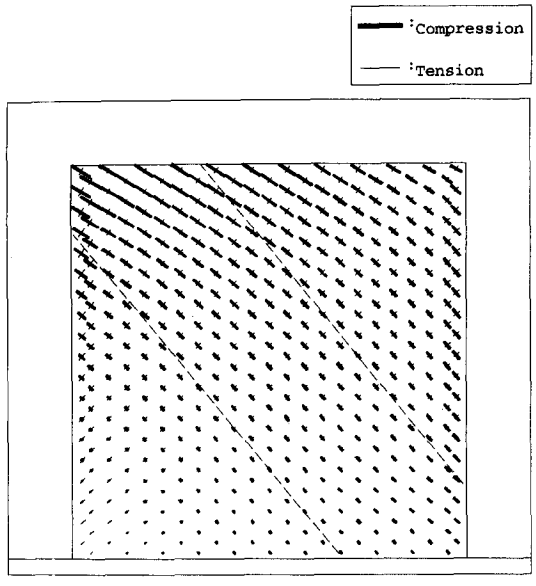

Fig. 12 Principal stress distribution of masonry wall (cracking and separation neglected; the dash lines define the effective region of the equivalent diagonal strut).

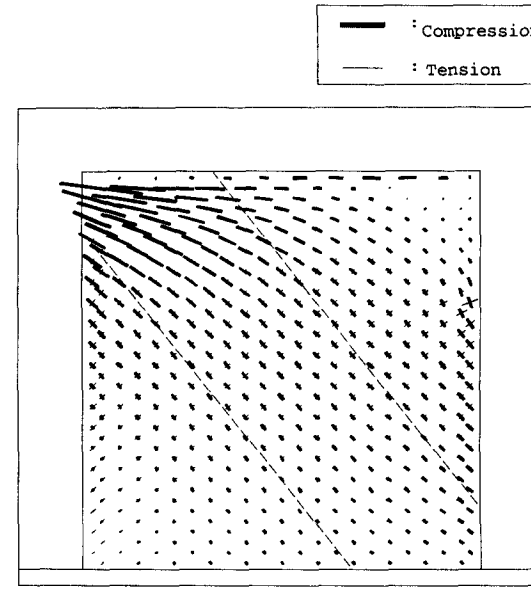

Fig. 13 Principal stress distribution of masonry wall (cracking and separation neglected; the dash lines define the effective region of the equivalent diagonal strut).

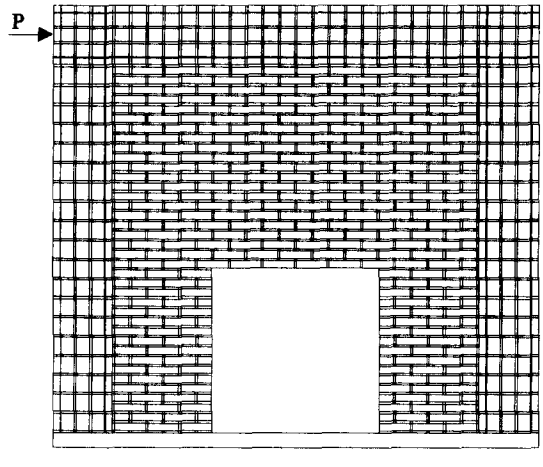

Fig. 14 Element mesh of infilled frame with opening.

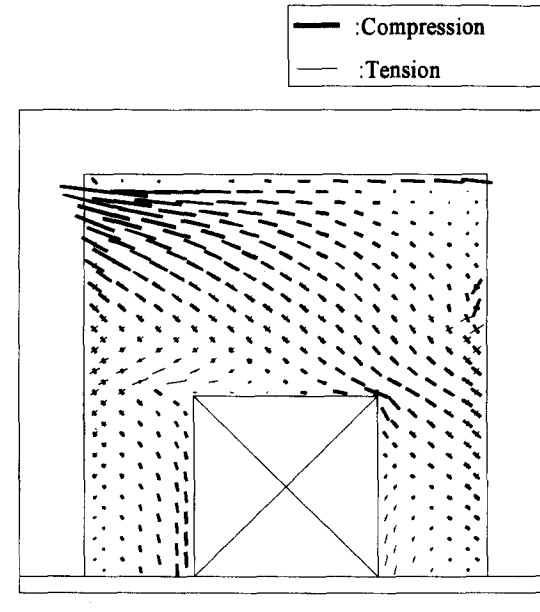

Fig. 15 Principal stress distribution of masonry wall (cracking and separation considered)

frame, and its distribution of principal stress is shown in Fig. 15. The cracking and separation of masonry wall are considered. It is found that the stress distribution becomes more complicated

and there is stress concentration around the corner of the opening. The cracking and separation phenomena make the principal direction of masonry wall no longer uniform and cause multiple regions of stress distribution. According to the principal stress distribution shown in Figs. 13 and 15, it is noted that the approximate equivalent strut (Smith 1966) sounds inapplicable for the masonry wall with separation or opening. The equivalent multiple struts (Thiruvengadam 1985) seem more appropriate for that type of masonry wall.

4. Conclusions

The modified DDA method is proposed to study the structural behaviors of reinforced concrete frames with masonry walls. An interface element is developed and it is incorporated into DDA to analyze the continuous and discontinuous behaviors of the masonry structure. The numerical solutions are verified first by being compared with previous research and they possess satisfactory agreement with each other. The proposed method is demonstrated to be appropriate for the analysis of masonry and reinforced concrete structures. Then the structural behavior and stress distribution of a reinforced concrete frame with a masonry wall subjected to a horizontal force are studied. The numerical results show that the behavior of the masonry structure is highly influenced by the failure of mortar. On the basis of the distribution of principal stress of the masonry wall in the reinforced concrete frame, the equivalent strut (Smith 1966) can be approximately substituted for the masonry wall without separation and opening. However, application of the equivalent strut to the masonry wall with separation and opening needs further study. The equivalent multiple struts (Thiruvengadam 1985) sound more appropriate for the masonry walls with separation or opening.

Acknowledgements

This study is supported by the National Science Council of Republic of China under grant No. NSC84-2621-P006-009B.

References

Abrams, D.P. and Paulson, T.J. (1991), "Modeling earthquake response of masonry building structures", *ACI Structural Journal*, July-August, 475-485.

Achyutha, H., Jagadish, R., Rao, P.S. and Rahman, S.S. (1986), "Finite element simulation of the elastic behavior of infilled frames with openings", *Computers & Structures*, **23**(5), 685-696.

Ali, S.S. and Page, A.W. (1988), "Finite element model for masonry subjected to concentrated loads", *Journal of Structural Engineering, ASCE*, **114**(8), 1761-1784.

Chang, C.T. (1994), "Nonlinear dynamic discontinuous deformation analysis with finite element meshed block system", Ph. D. Dissertation, Department of Civil Engineering, University of California, Berkeley, USA.

Chen, W.F. and Saleeb, A.F. (1982), "Constitutive equations for engineering materials", *Elasticity and Modelling*, **1**, 303-324, Wiley-Interscience, New York.

Clough, R.W., Gulkan, P., Mayes, R.L. and Manos, G.C. (1990), "Seismic testing of single-story masonry house: Part 2", *Journal of Structural Engineering, ASCE*, **116**(1), 257-274.

Cundall, P.A. (1971), "A computer model for simulating progressive, large scale movements in block rock systems", *Symposium of International Society of Rock Mechanics*, Nancy, France, paper II-8.

Cundall, P.A. and Hart, R.D. (1989), "Numerical modelling of discontinua", *Proceedings of the 1st U.S. Conference on Discrete Element Methods*, Golden, Colorado, G.G.W. Mustoe, M. Henriksen and H.P. Huttelmaier, eds., 17p.

Dawe, J.L. and Seah, C.K. (1989a), "Behaviour of masonry infilled steel frames", *Canadian Journal of Civil Engineering*, **16**, 865-876.

Dawe, J.L. and Seah, C.K. (1989b), "Masonry infilled steel frames subject to dynamic load", *Canadian Journal of Civil Engineering*, **16**, 877-885.

El Haddad, M.H. (1991), "Finite element analysis of infilled frames considering cracking and separation phenomena", *Computers & Structures*, **41**(3), 439-447.

El Shabrawi, A. and Verdel, T. (1995), "Modelling of ancient masonry structures by the distinct element method under dynamic loads", *Structural Studies of Historical Buildings IV-Volume 2: Dynamic, Repairs & Restoration*, Editors: C.A. Brebbia, B. Leftheris, Computational Mechanics Publications, Southampton, UK.

Gulkan, P., Clough, R.W., Mayes, R.L. and Manos, G.C. (1990), "Seismic testing of single-story masonry house: Part 1", *Journal of Structural Engineering, ASCE*, **116**(1), 235-256.

Haider, S. (1996), "In-plane cyclic response of reinforced concrete frames with unreinforced masonry infills", Ph. D. Dissertation, Department of Civil Engineering, Rice University, USA.

Ke, T.C. (1993), "Simulated testing of two dimensional heterogeneous and discontinuous rock masses using discontinuous deformation analysis", Ph. D. Dissertation, Department of Civil Engineering, University of California, Berkeley, USA.

Liauw, T.C. (1972), "An approximate method of analysis for infilled frames with or without opening", *Building Science*, **7**, 233-238.

Lin, C.T. (1995), "Extensions to the discontinuous deformation analysis for jointed rock masses and other blocky systems", Ph. D. Dissertation, Department of Civil, Environmental and Architectural Engineering, University of Colorado, USA.

Lotfi, H.R. and Shing, P.B. (1991), "An appraisal of smeared crack models for masonry shear wall analysis", *Computers & Structures*, **41**(3), 413-425.

May, I.M. and Naji, J.H. (1991), "Nonlinear analysis of infilled frames under monotonic and cyclic loading", *Computer & Structures*, **38**(2), 149-160.

Mehrabi, A.B. (1994), "Behavior of masonry-infilled reinforced concrete frames subjected to lateral loadings", Ph. D. Dissertation, University of Colorado at Boulder, USA.

Papia, M. (1988), "Analysis of infilled frames using a coupled finite element and boundary element solution scheme", *International Journal for Numerical Methods in Engineering*, **26**, 731-742.

Saneinejad, A. and Hobbs, B. (1995), "Inelastic design of infilled frames", *Journal of Structural Engineering*, **121**(4), 634-650.

Shi, G.H. (1988), "Discontinuous deformation analysis: A New Numerical Model for the Statics and Dynamics of Block Systems", Ph. D. Dissertation, Department of Civil Engineering, University of California, Berkeley, USA.

Shyu, K. (1993), "Nodal-based discontinuous deformation analysis", Ph. D. Dissertation, Department of Civil Engineering, University of California, Berkeley, USA.

Smith, B.S. (1966), "Behavior of square infilled frames", *Journal of Structure Division, ASCE*, **92**(ST1), 381-403.

Suidan, M. and Schnobrich, W.C. (1973), "Finite element analysis of reinforced concrete", *Journal of Structural Division, ASCE*, **99**(ST10), 2109-2122.

Thiruvengadam, V. (1985), "On the natural frequencies of infilled frames", *Earthquake Engineering and Structural Dynamics*, **13**, 401-419.